

## CHAPTER 3

### THE AMPHIPHILIC CHARACTER OF THE HYDRATED PROTON IN METHANOL-WATER SOLUTIONS

Reprinted with permission from the American Chemical Society  
(Petersen, M.K., Voth, G.A., 2006. J. Phys. Chem. B 110, 7085-7089)

## Amphiphilic Character of the Hydrated Proton in Methanol–Water Solutions

Matt K. Petersen and Gregory A. Voth\*

Center for Biophysical Modeling and Simulation and Department of Chemistry, University of Utah,  
315 South 1400 East, Room 2020, Salt Lake City, Utah, 84112-0850

Received: February 1, 2006; In Final Form: March 3, 2006

The hydrated proton was studied in methanol–water solutions of varying methanol concentrations using the multistate empirical valence bond simulation method. Amphiphile-like behavior of the hydrated proton was noted from its anisotropic association with the methanol methyl groups. Molecular length immiscibility was also characterized through the enumeration of water and protonated water clusters. Excess proton diffusion was calculated across the varying methanol concentrations and found to be in good agreement with experiment after correcting for nuclear quantum effects.

### Introduction

It has been demonstrated previously through computer simulation that the hydrated proton exhibits an interesting “amphiphilic” character in water clusters<sup>1,2</sup> and near the water liquid/vapor interface.<sup>3</sup> Although the degree of surface enhancement seems to be potential-energy-function-dependent,<sup>4,5</sup> there is compelling experimental support<sup>6–8</sup> for the surface enrichment observed in both empirical force field<sup>3,9</sup> and *ab initio* simulations.<sup>1,2</sup> In this letter we investigate the amphiphilic behavior of the hydrated proton in methanol–water solutions and show that the previously noted amphiphilic behavior observed for the aqueous liquid/vapor interface generalizes to the anisotropic association of the hydronium ion with the methanol hydrophobic methyl groups.

Studies of methanol–water solutions, both experimental<sup>10</sup> and computational,<sup>11–13</sup> provide support for a molecular immiscibility, that is, an incomplete mixing at molecular length scales. Herein we also examine the relationship between this immiscibility and the clustering behavior of both water and the hydrated excess proton and report transport properties across a range of methanol/water concentrations. The diffusion of the hydrated proton is shown to be related to its average coordination and to the relative concentrations of Eigen and Zundel solvation structures.

Previous computer simulations have shown that the hydrated excess proton displays what is appropriately described as amphiphile-like behavior near the water liquid/vapor and liquid/vacuum interface. This behavior is analogous to that of a methanol molecule in both neat and methanol–water solutions at the liquid/vapor interface. Computer simulation of neat liquid methanol<sup>25</sup> and subsequent experimental data (incidentally, the first surface vibrational spectrum of a neat liquid<sup>26</sup>) indicate that the methanol molecule preferentially orients the hydrophobic methyl group away from the liquid of the liquid/vapor interface. Simulations of methanol–water solutions also dem-

onstrate methanol surface enrichment and preferential orientation of the methyl group at liquid/vapor interfaces,<sup>27</sup> both of which have been verified through experiment.<sup>7,28</sup>

The amphiphilic quality of the hydrated proton has been attributed to the highly anisotropic solvation of the hydronium ion due to the exclusion of water from the first solvation shell on the “lone-pair” side of the cation.<sup>3</sup> One would therefore naturally question if this previously demonstrated amphiphile-like behavior of the hydrated proton seen at the water/vacuum interface is also exhibited in other mixed dielectric environments, such as water–amphiphile mixtures.

### Simulation Details

The present simulation results are based on 5 ns of microcanonical trajectories for seven methanol–water solutions of varying methanol concentrations. Each system consisted of 343 total molecules under periodic boundary conditions at the experimental density for a given concentration in ratios of 0.29, 9.91, 30.0, 50.1, 70.0, 90.1, and 99.7% methanol. The OPLS-AA force field<sup>14</sup> was used to describe the methanol potential, while the water potential was adopted from the water model in the MS-EVB2 force field.<sup>15</sup> The parameters for the Lennard-Jones interaction were obtained using the standard Lorentz–Berthelot mixing rules, and all electrostatic interactions were treated with the Ewald summation method.

The initial equilibration phase consisted of 500 ps of standard molecular dynamics (MD) for each mixture, alternating between the NPT (constant number, pressure, and temperature) and NVT (constant number, volume, and temperature) ensembles at 100 ps intervals with the temperature and pressure set to the desired final values of 300 K and 1 atm, respectively. A single excess proton was then added to the final configuration, and the system was further equilibrated under NVT conditions with the inclusion of the MS-EVB2 potential for describing the hydrated proton. The resulting configurations were then used to initiate constant NVT trajectories from which five starting configurations were taken at 10 ps intervals for each solution concentration. These five configurations were used to initiate five

\* Author to whom correspondence should be addressed. E-mail: voth@chem.utah.edu.

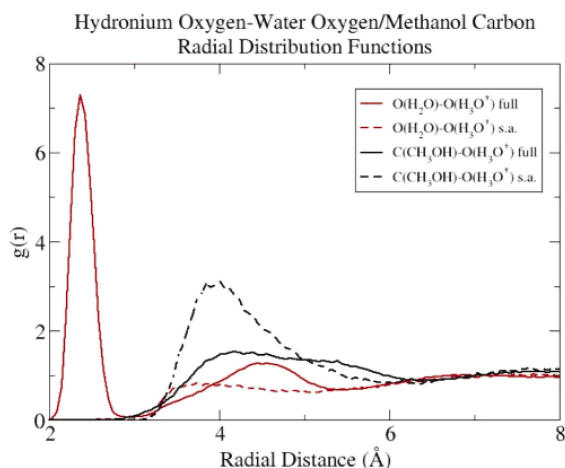


**Figure 1.** Red Curves: Radial distribution functions between water and hydronium oxygen: full radial distribution (red solid line) and the radial distribution restricted to a  $\pi$  steradian solid angle with its apex centered about the lone-pair side of the hydronium ion (red dashed line). Black curves: Radial distribution functions between methanol carbon and hydronium oxygen: full radial distribution (black solid line) and the radial distribution restricted to a  $\pi$  steradian solid angle with its apex centered about the lone-pair side of the hydronium ion (black dashed line).

independent 1 ns microcanonical trajectories resulting in a total of 5 ns of data for each of the solution concentrations.

Protonated methanol (methoxonium) was *not* included in the present multistate empirical valence bond (MS-EVB) description. However, we believe this to be problematic for only the most methanol-rich solutions. Guss and Kolthoff have shown<sup>16</sup> through a direct titration of methoxonium in methanol-rich solutions that the protonation of water is strongly favored over methanol. This is in good agreement with the more recent measurements<sup>17,18</sup> that show that for methanol-rich solutions, 90% methanol, for example, protonated water predominated by a full order of magnitude and for low methanol content, say 10%, the protonated water concentration dominates that of protonated methanol by more than 3 orders of magnitude. Additionally, several studies of excited-state photoacid proton transfer into water–methanol solutions have established water as the proton acceptor for nearly the full methanol–water composition range.<sup>19–23</sup> The solvation structure of the hydrated proton is still a point of contention and will be discussed in more detail in the clustering segment of the Results section.

A recent *ab initio* molecular dynamics (AIMD) study of a protonated 50% methanol–water solution has reported branching ratios of proton-transfer reactions among water and methanol that indicate a ratio of approximately 2:3, somewhat favoring the protonation of water.<sup>24</sup> It is unclear if the relatively large concentration of protonated methanol is a direct result of the electronic density functional used in the AIMD or possible difficulties in equilibration of the demanding AIMD simulations. Either way, the AIMD results tend to be in substantial disagreement with the experimental results described above.

## Results

**Amphiphilic Hydrated Proton Behavior.** Figure 1 depicts the hydronium oxygen–water oxygen and hydronium oxygen–methyl carbon radial distribution functions for the 30% methanol solution. Full radial distribution functions were calculated as well as partial distributions that were restricted to a  $\pi$  steradian

solid angle with the apex formed from the vector extending from the hydronium hydrogen center of mass through the hydronium oxygen. The first solvation shell of the hydronium cation is filled exclusively by three strongly solvating water molecules (solid red line) as shown by the sharp peak at approximately 2.5 Å. In contrast, the methyl carbon curve (solid black line) shows no density within the first hydronium solvation shell and rises no further than the average bulk atomic density within the second solvation shell, at  $\sim 4$  Å.

The restricted radial distribution functions display a remarkably different trend. The red dashed line is the restricted distribution for hydronium oxygen–water oxygen pairs. The anisotropic solvation is evident, but most striking is the lack of significant density in the region of the second solvation shell. Not only are water molecules excluded from the first solvation shell on the lone-pair side of the hydronium ion, there is apparently a significant depletion in the second solvation shell as well. The restricted distribution for the methyl carbon–hydronium oxygen pair (black dashed line) is, however, quite different from the hydronium–water radial distributions. While water is depleted in this lone-pair region, the methyl carbon density is found to be in excess of 3 times the average bulk value. This preferential association is seen in Figure 2a.

This behavior described in the previous paragraph is more clearly understood by viewing the spatial distribution function (Figure 2b). All isosurfaces are for regions where the atomic densities are 3 times or greater than the average uniform atomic densities. The water oxygen density (red) of the first two solvation shells is well-structured. The first solvation shell is responsible for the solid padlike structures along the hydronium oxygen–hydrogen bond; the second shell is evident in the ringlike structures just behind the first. The lone-pair side of the cation is occupied exclusively by the methyl carbon density (cyan). Additionally, a small volume of carbon density is located below the hydronium hydrogen atoms. The hydronium cation clearly exhibits amphiphile-like directional hydrophilic/hydrophobic solvation; water is strongly coordinated along each hydrogen but completely displaced by the methyl groups in the hydrophobic cap region on the lone-pair side of the cation.

**Clustering.** Water clusters were defined as contiguous groups of water molecules wherein each member of the cluster had an oxygen–oxygen distance of 3.5 Å or less from any other member of the cluster. Figure 3 displays the water cluster size probability distribution and the protonated water cluster size probability distribution for the 70% methanol solution. The probability is defined as the chance of finding a given water molecule or protonated water molecule in a cluster of size  $n$ . At this solution concentration, clusters composed of a single water molecule predominate with a smooth decay in probability as cluster size increases. The clustering behavior is in qualitative agreement with that observed by Dixit et al.<sup>12</sup> for larger clusters. However, for cluster sizes  $n = 1–3$  there is a statistically significant difference in that Dixit et al. observed clusters of  $n = 3$  as the predominant cluster size.

We should note that for the more water-rich solutions enumeration of the cluster distribution becomes problematic. As water content is increased the hydrogen bond network becomes progressively more extensive. In the most water-rich compositions, clusters that contain nearly every water molecule in the simulation will dominate, producing a bimodal cluster distribution skewed toward these very large clusters. Investigations of larger systems indicate that the distribution of smaller clusters remains nearly unchanged by increasing the system size.

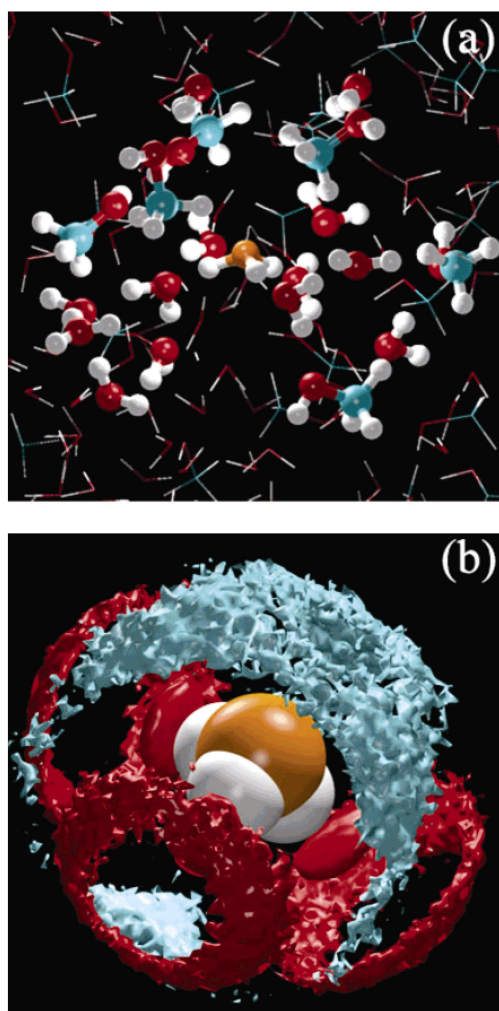


**Figure 2.** (a) Typical configuration from the 30% methanol solution with the hydronium (orange) seen to prefer the interface with the methanol methyl groups (cyan). (b) Isodensity surfaces of water oxygen (red) and methanol carbon (cyan) about the hydronium ion for points containing 3 times the average atomic densities.

Apparently very large clusters are in effect joined into even larger clusters as an artifact of the periodic boundary conditions.

The protonated cluster distribution differs significantly from the total water cluster distribution in that no single-molecule clusters, i.e.,  $(\text{H}_2\text{O})\cdot\text{H}^+$ , were observed and that the most probable protonated cluster sizes grouped about  $n = 12$ . This is due to the much stronger water solvation of the hydronium compared with that of a water molecule. The coordination of the hydronium ion remains very close to its bulk value of three strongly coordinating water molecules, i.e.,  $\sim 2.7$ , while the water molecules' coordination is reduced from the average bulk value of approximately 4 water molecules to an average of 1.3. Water molecules form another 2.0 hydrogen bonds to neighboring methanol molecules for an overall reduction from the average  $\sim 4$  hydrogen bonds of bulk water to 3.3 hydrogen bonds in the 70% methanol solution. Interestingly, the total coordination for methanol molecules is increased from the approximate 2 hydrogen bonds of bulk methanol. The number of hydrogen bonds to neighboring methanol molecules is reduced to 1.4, but another 0.9 hydrogen bonds are formed to water molecules, thus

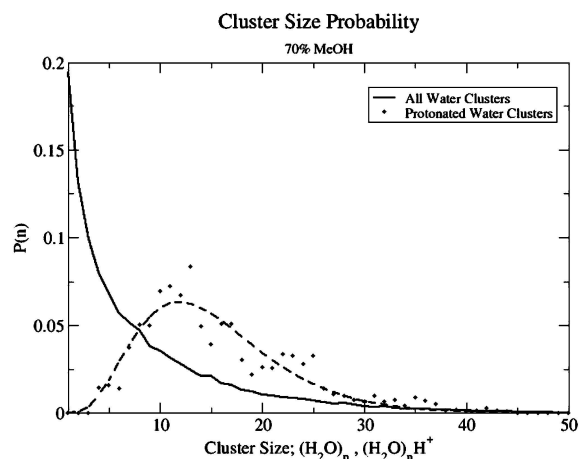


**Figure 3.** Solid line: The probability of finding a given water molecule in a cluster of size  $n$ . Dashed line: The probability of finding the water molecule in a protonated cluster of size  $n$ .

increasing the overall coordination to 2.3. These coordinating trends were similarly observed by Dixit et al.<sup>12</sup>

Excited-state photoacid proton-transfer reactions in methanol–water solutions have proven to be useful probes of solvent inhomogeneity in methanol–water solutions. While there is reasonable consensus that water is the proton acceptor for solution concentrations below  $\sim 90\%$  (w) methanol, the nature of the solvation of the aqueous protonic core is in dispute. Early studies using Markov random walk theory identified the proton acceptor as  $(\text{H}_2\text{O})_{4\pm 1}$ , arguing that at high methanol concentrations the proton-transfer reaction was diffusion-controlled.<sup>19</sup> Fillingim et al. have also identified the  $\text{H}_9\text{O}_4^+$  cluster through fitting 1-naphthol and 2-naphthol decay rates.<sup>20</sup>

However, a more exhaustive study<sup>23</sup> employing photoacids of varying strengths have shown that the water-dependent contribution to the dissociation constant is photoacid-dependent and therefore more likely a probe of the contact ion pair (CIP) structure and not the bulk proton solvation structure, suggesting that the CIP exists as a water-molecule-separated  $\text{H}_3\text{O}^+$  ion for the most acidic photoacids. This explanation is consistent with previous observations of concentrated strong acid water simulations using the MS-EVB2 potential.<sup>29</sup>

Pines and Fleming have attempted to elucidate the nature of bulk protonic solvation by measuring proton dissociation rates for a given photoacid in a range of water/organic solvents and compositions, correlating the maximum dissociation rate along the solvent composition range and the organic solvent proton affinity.<sup>21</sup> While the exact composition of the proton solvation shell was unresolved, these authors suggest a pair interaction between the organic solvent through a direct hydrogen bond to the aqueous core of the proton solvation shell, effectively withdrawing proton density and indirectly increasing the associated water molecules' proton affinity. The maximum observed proton dissociation rate in methanol–water solutions suggests an optimal cosolvent molecular ratio of 1:1.

By directly inspecting the restricted and full radial distribution functions for the 50% methanol solutions we are able to elucidate the nature of this cosolvation for our simulated systems. The hydronium ion is immediately solvated by three ligands,  $\sim 2.8$  water molecules, and  $\sim 0.2$  methanol molecules, in an Eigen-like configuration. This nominally aqueous core is solvated by an additional  $\sim 5.5$  water molecules and  $\sim 4.5$  methanol molecules through hydrogen bonds to the three



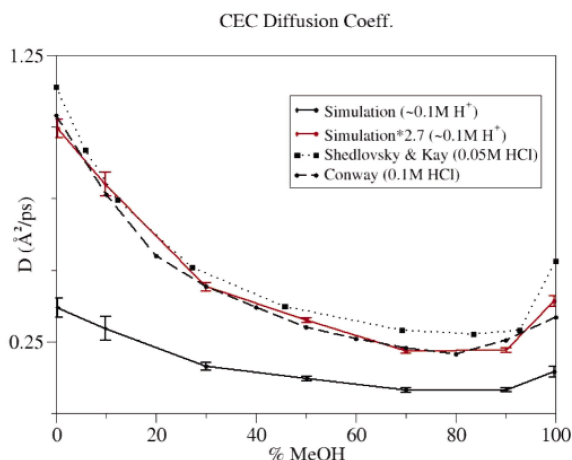


**Figure 4.** Experimental (dot and dashed, black)<sup>34,35</sup> and simulation (solid, black and red) excess proton diffusion values for varying methanol/water concentrations. The offset between the simulated and the experimental curves is largely due to a nuclear quantum correction (which could be as large as a factor of  $\sim 2.7$ , solid red line) not included in the classical MS-EVB simulations.

immediately solvating molecules. Additionally,  $\sim 3$  methanol molecules solvate the hydrophobic cap region of the hydronium while hydrogen bonding to an average of  $\sim 0.5$  water molecules. So, while the solvated aqueous core has an ostensibly 1:1 cosolvent molecular ratio, the aqueous core is well-structured and solvated through two disparate water–organic solvent pair interactions, an Eigen-like aqueous core solvated more or less equally by hydrogen bonded water/methanol molecules and a hydrophobic cap region solvated by a trio of methanol methyl groups.

**Excess Proton Diffusion.** Diffusion of the center of excess charge (CEC),<sup>15</sup> or the excess proton defect, was calculated across the range of simulated concentrations (Figure 4). While the absolute diffusion of the excess charge is less than the experimental diffusion, the diffusion trend is accurately reproduced; for all concentrations, the diffusion of the CEC is approximately one-third of the experimental value (in Figure 4, the solid red line shows the corrected curve). This factor is largely due to a quantum nuclear correction,<sup>30,31</sup> which is not included in these classical MS-EVB simulations.

Since the total diffusion of the CEC involves both the passing of the charge defect through bond formation/cleavage, i.e., Grotthuss shuttling,<sup>32,33</sup> and conventional vehicular diffusion during the CEC's transient residence on a given molecule, an estimate of these contributions can be found by comparing the CEC diffusion to that of the water. The CEC diffusion in the 0% methanol solution was  $110 \pm 5\%$  of the water diffusion; in the 70% it was  $40.7 \pm 0.7\%$ . The decrease in the diffusion ratio is likely due to the reduced coordination of the waters solvating the hydronium ion. While the hydronium ion remains in nominally 3-fold coordination in the 70% solution, the water molecules directly solvating it have a significantly reduced coordination. Proton transfer through bond formation/cleavage with a first solvation shell water molecule would result in an incompletely solvated hydronium ion (a structure that is energetically unfavorable compared to the former solvation environment, thus reducing the likelihood of diffusion through this mechanism). However, for the 90% methanol solutions the coordination of the hydronium ion is reduced to 2.2 solvating water molecules. This reduction in coordination is accompanied by an increase in the water–CEC diffusion ratio to  $46.0 \pm 0.7\%$ .

Since the environment in this reduced coordination state is more similar to the poorly solvated first solvation shell, the penalty for diffusion via Grotthuss shuttling is consequently reduced. It is also similar to the quasi-one-dimensional “proton wire” of a protonated linear chain of water molecules.

A comparison of the MS-EVB state amplitudes suggests Eigen-like solvation is increasingly favored as methanol concentration increases. As presumably any proton-transfer event must involve a transient Zundel moiety, it is not surprising that the Grotthuss shuttling mechanism has a diminished contribution to the total CEC diffusion at higher methanol concentrations. The trend continues until the 90% methanol solution, where Zundel-like solvation begins to become more prominent with the reduction in coordination of the hydronium. In the 90% methanol solution, proton “hopping” occurs more frequently than was observed for 70% methanol and is directed along water-wire-like clusters and rings. It is important to note that the excluded protonated methanol states may significantly impact the diffusion rate at concentrations of 90% methanol or greater, but it is unclear what effects the inclusion of these states may have. Perhaps the inclusion of these states may stabilize the excess proton, thus diminishing diffusion or perhaps enhance it through their participation in the Grotthuss shuttling mechanism. This will be the topic of future research.

## Conclusions

The amphiphilic character of the hydrated proton observed in previous simulations of water liquid–vacuum interfaces was found to extend to association with hydrophobic groups in water–methanol mixtures. Preliminary results for the methanol–water solution liquid/vapor interface (not given here) also suggest that the hydronium ion seeks the methanol-rich region near the interface. These results are to be distinguished from the conclusions drawn in the study of Morrone et al.,<sup>24</sup> where they found significant residence of the proton defect in methanol-rich regions, indeed frequently residing on a methanol molecule, in apparent disagreement with experiment. We have instead identified a distinctly different phenomenon. The hydrated proton was found to have an asymmetric amphiphile-like solvation through hydrophilic interactions (hydrogen bonds) with both water and the organic solvent and “hydrophobic” interactions between the aqueous core and the hydrophobic groups of the organic solvent. Further study of this phenomenon will be the focus of ongoing work.

The molecular immiscibility, or clustering behavior, previously observed in the Monte Carlo simulations of Dixet et al.<sup>12</sup> was seen for methanol–water concentrations ranging from 0 to 100% methanol. Additionally, a distribution distinct from the overall water cluster distribution was observed for proton-containing clusters, distinguished by depletion in the probability of observing lighter clusters. Diffusion of the excess proton was characterized for the range of concentrations, and it was found that the Grotthuss-like hopping is generally diminished as methanol content increases. However, upon a reduction in the average hydronium coordination at 90% methanol content, the hopping contribution to the total excess proton diffusion increased.

Although still in need of direct experimental confirmation and further simulation studies using increasingly accurate models, the results presented in this communication suggesting an “amphiphilic” behavior of the excess hydrated proton in mixed water–amphiphile solutions have significant implications that will require continued exploration.

**Acknowledgment.** This research was supported by a grant from the National Science Foundation (CHE-0317132). We thank Dr. Kim Wong and Mr. Mark Maupin for their critical reading of the manuscript.

# References and Notes

- (1) Iyengar, S. S.; Day, T. J. F.; Voth, G. A. *Int. J. Mass Spectrosc.* **2005**, *241*, 197.
- (2) Iyengar, S. S.; Petersen, M. K.; Burnham, C. J.; Day, T. J. F.; Voth, G. A. *J. Chem. Phys.* **2005**, *123*, 084309.
- (3) Petersen, M. K.; Iyengar, S. S.; Day, T. J. F.; Voth, G. A. *J. Phys. Chem. B* **2004**, *108*, 14804.
- (4) Mucha, M.; Frigato, T.; Levering, L. M.; Allen, H. C.; Tobias, D. J.; Dang, L. X.; Jungwirth, P. *J. Phys. Chem. B* **2005**, *109*, 7617.
- (5) Dang, L. X. *J. Chem. Phys.* **2003**, *119*, 6351.
- (6) Shultz, M. J.; Schnitzer, C.; Simonelli, D.; Baldelli, S. *Int. Rev. Phys. Chem.* **2000**, *19*, 123.
- (7) Miranda, P. B.; Shen, Y. R. *J. Phys. Chem. B* **1999**, *103*, 3292.
- (8) Radüge, C.; Pflumio, V.; Shen, Y. R. *Chem. Phys. Lett.* **1997**, *274*, 140.
- (9) Burnham, C. J.; Petersen, M. K.; Day, T. J. F.; Iyengar, S. S.; Voth, G. A. *J. Chem. Phys.* **2006**, *124*, 024327.
- (10) Holden, C. A.; Hunnicutt, S. S.; Sanchez-Ponce, R.; Craig, J. M.; Rutan, S. C. *Appl. Spectrosc.* **2003**, *57*, 483.
- (11) Dougan, L.; Bates, S. P.; Hargreaves, R.; Fox, J. P.; Crain, J.; Finney, J. L.; Réat, V.; Soper, A. K. *J. Chem. Phys.* **2004**, *121*, 6456.
- (12) Dixit, S.; Crain, J.; Poon, W. C. K.; Finney, J. L.; Soper, A. K. *Nature* **2002**, *416*, 829.
- (13) Allison, S. K.; Fox, J. P.; Hargreaves, R.; Bates, S. P. *Phys. Rev. B* **2005**, *71*, 024201.
- (14) Kaminski, G.; Jorgensen, W. L. *J. Phys. Chem.* **1996**, *100*, 18010.
- (15) Day, T. J. F.; Soudackov, A. V.; Cuma, M.; Schmitt, U. W.; Voth, G. A. *J. Chem. Phys.* **2002**, *117*, 5839.
- (16) Guss, L. S.; Kolthoff, I. M. *J. Am. Chem. Soc.* **1940**, *62*, 1494.
- (17) DeLisi, R.; Goffredi, M. *Electrochim. Acta* **1971**, *16*, 2181.
- (18) Kondo, Y.; Tokura, N. *Bull. Chem. Soc. Jpn.* **1972**, *45*, 818.
- (19) Lee, J.; Robinson, G. W.; Webb, S. P.; Philips, L. A.; Clark, J. H. *J. Am. Chem. Soc.* **1986**, *108*, 6538.
- (20) Fillingim, T. G.; Luo, N.; Lee, J.; Robinson, G. W. *J. Phys. Chem.* **1990**, *94*, 6368.
- (21) Pines, E.; Fleming, G. R. *J. Phys. Chem.* **1991**, *95*, 10448.
- (22) Agmon, N.; Huppert, D.; Masad, A.; Pines, E. *J. Phys. Chem.* **1991**, *95*, 10407.
- (23) Solntsev, K. M.; Huppert, D.; Agmon, N.; Tolbert, L. M. *J. Phys. Chem. A* **2000**, *104*, 4658.
- (24) Morrone, J. A.; Haslinger, K. E.; Tuckerman, M. E. *J. Phys. Chem. B* **2006**, *110*, 3712.
- (25) Matsumoto, M.; Kataoka, Y. *J. Chem. Phys.* **1989**, *90*, 2398.
- (26) Superfine, R.; Huang, J. Y.; Shen, Y. R. *Phys. Rev. Lett.* **1991**, *66*, 1066.
- (27) Matsumoto, M.; Takaoka, Y.; Kataoka, Y. *J. Chem. Phys.* **1993**, *98*, 1464.
- (28) Raina, G.; Kulkarni, G. U.; Rao, C. N. R. *J. Phys. Chem. A* **2001**, *105*, 10204.
- (29) Petersen, M. K.; Wang, F.; Blake, N. P.; Metiu, H.; Voth, G. A. *J. Phys. Chem. B* **2005**, *109*, 3727.
- (30) Schmitt, U. W.; Voth, G. A. *J. Chem. Phys.* **1999**, *111*, 9361.
- (31) Schmitt, U. W.; Voth, G. A. *Chem. Phys. Lett.* **2000**, *36*.
- (32) Grotthuss, C. J. T. d. *Ann. Chim. (Paris)* **1806**, *58*, 54.
- (33) Danneel, H. Z. *Elektrochem.* **1905**, *11*, 249.
- (34) Shedlovsky, T.; Kay, R. L. *J. Phys. Chem.* **1956**, *60*, 151.
- (35) Conway, B. E. *J. Chem. Phys.* **1956**, *24*, 834.